ISSN 0016-7029, Geochemistry International, 2007, Vol. 45, No. 2, pp. 105–122. © Pleiades Publishing, Ltd., 2007.
Original Russian Text © V.I. Kovalenko, V.B. Naumov, A.V. Girnis, V.A. Dorofeeva, V.V. Yarmolyuk, 2007, published in Geokhimiya, 2007, No. 2, pp. 131–149.

Volatiles in Basaltic Magmas of Ocean Islands and Their Mantle Sources: I. Melt Compositions Deduced from Melt Inclusions and Glasses in the Rocks

V. I. Kovalenko[a], V. B. Naumov[b], A. V. Girnis[a], V. A. Dorofeeva[b], and V. V. Yarmolyuk[b]

[a] *Institute of the Geology of Ore Deposits, Petrography, Mineralogy, and Geochemistry, Russian Academy of Sciences, Staromonetnyi per. 35, Moscow, 119017 Russia*
e-mail: vik@igem.ru

[b] *Vernadsky Institute of Geochemistry and Analytical Chemistry, Russian Academy of Sciences, ul. Kosygina 19, Moscow, 119991 Russia*
e-mail: naumov@geokhi.ru

Received June 15, 2005

Abstract—Statistical analysis of a data bank of the compositions of glasses and melt inclusions in minerals from ocean-island basalts. The initial database contains more than 45000 published analyses of ocean-island igneous rocks from around the world. Much attention was given to the contents of volatiles (H_2O, Cl, F, and S) and their ratios to one another and to nonvolatile components of close incompatibility (Ti, P, K, and Ce). The average compositions of melt inclusions are similar to those of glasses of the rocks, including volatiles, with consideration for a somewhat higher degree (by approximately 20%) of the differentiation of glasses. The average compositions of ocean-island melts differ from those of mid-ocean basalts in having wider variations and elevated contents of some of the most incompatible elements (Sr, Nb, Ta, Ba, U, Th, and others), as well as H_2O, F, and Cl. Based on the correlation of volatiles to one another and to incompatible elements, three groups of ocean-island basalts are distinguished: (I) low-K, P, Ti magma compositions approximating mid-ocean ridge magmas, (II) high-K, Ce, P, and Ti magmas that resemble continental rift magmas but differ from them in low H_2O content, and (III) high-K, H_2O, Ce, P, and Ti magmas close to continental rift magma. All three types of the melts were found only in the Hawaiian Archipelago, whereas other ocean islands are dominated by any one of these types. The distinguished melt types presumably reflect the differences (heterogeneity) in the compositions of the sources.

DOI: 10.1134/S0016702907020012

INTRODUCTION

Reliable estimates of the compositions of natural magmas formed in different geodynamic settings can be obtained by studying primary melt inclusions in minerals and quench glasses in rocks. These data are of special importance in estimating the contents of volatiles, which are partially removed during magma eruption or crystallization. We have long been developing a database of magma compositions, which consists of analyses of primary melt inclusions and quench glasses. The database was used to estimate the average compositions of melts formed in various geodynamic settings [1, 2]. The database presently contains more than 260000 analyses for volatile, major, and trace elements (73 elements in total) in melt inclusions and quench glasses from magmatic rocks of various geodynamic settings. This paper addresses the problem of estimating the compositions of oceanic-island and oceanic-plateau magmas and their sources with the aim of constructing a compositional model of mantle plumes. Much attention was paid to the contents of volatiles (H_2O, Cl, F, and S) and incompatible elements (K, Ce, Ti, P, and others), which behave as volatiles during the derivation of mantle magmas. Since a great number of data was accumulated, the investigation results were presented in two papers. The first paper is focused on the average compositions of melts estimated from data on glasses in inclusions and rocks and on the compositional variations related to the existence of different sources. The second paper will be devoted to the possible compositions of mantle sources and the compositional structure of mantle plumes.

FACTUAL MATERIAL

Our database now contains about 45000 analyses of glasses from inclusions and rocks of ocean islands and plateau compiled from 108 papers. Most of the analyses were borrowed from 50 publications, each containing more than 20 analyses [3–52]. Table 1 lists average contents of major, volatile, and rare elements, including 800 determinations of H_2O, 1385 determinations of Cl,

Table 1. Average contents of major, volatile, and trace elements in mineral melt inclusions and quenched glasses from ocean-island magmatic melts

Component	Melt inclusions			Quenched glasses			Component	Melt inclusions			Quenched glasses		
	n	arithm.	geom.	*n*	arithm.	geom.		*n*	arithm.	geom.	*n*	arithm.	geom.
SiO_2	1696	50.04	50.03	1751	50.40	50.39	V	107	195	192	155	312	317
		2.04	2.10–2.01		2.09	2.17–2.07			84	91–62		83	108–81
TiO_2	1635	2.03	1.56	1655	2.65	2.61	Cr	423	647	494	262	236	237
		1.02	1.09–0.64		0.62	0.68–0.53			776	963–327		194	310–134
Al_2O_3	1650	13.86	13.83	1655	13.87	13.86	Ni	55	383	334	262	172	140
		2.02	2.15–1.86		1.00	1.08–1.00			375	409–184		147	181–79
FeO	1684	9.93	9.90	1657	11.26	11.25	Sr	297	198	177	196	314	273
		2.28	2.64–2.08		1.18	1.41–1.24			199	334–115		273	312–145
MnO	1221	0.14	0.14	938	0.18	0.19	Y	186	13.1	12.8	175	27.6	27.6
		0.05	0.06–0.04		0.06	0.05–0.04			6.6	6.7–4.4		7.9	9.0–6.8
MgO	1684	8.43	8.39	1740	6.54	6.49	Zr	283	70.0	48.9	193	124	124
		2.32	2.85–2.13		1.46	1.77–1.40			80.5	145–36.6		70	80–49
CaO	1650	11.58	11.63	1655	10.99	10.95	Nb	156	10.9	9.3	168	18.1	10.8
		2.00	2.43–2.00		1.12	1.37–1.22			10.1	7.7–4.2		38.6	13.6–6.0
Na_2O	1635	2.22	2.20	1655	2.52	2.45	Ba	211	56.2	56.6	146	102	77.0
		0.58	0.55–0.44		0.74	0.64–0.51			63.8	155–42		172	184–54
K_2O	1600	0.48	0.48	1740	0.55	0.59	La	342	4.62	2.30	187	11.7	9.4
		0.49	0.68–0.28		0.56	0.42–0.25			6.99	5.30–1.61		18.9	12.2–5.3
P_2O_5	1336	0.26	0.26	1563	0.29	0.27	Ce	230	6.27	3.37	185	26.1	22.7
		0.21	0.34–0.15		0.21	0.13–0.09			13.8	5.15–2.04		27.6	24.9–11.9
H_2O	293	0.35	0.34	505	0.42	0.49	Nd	230	5.10	3.19	185	16.6	15.9
		0.36	0.71–0.23		0.34	0.45–0.23			8.84	3.76–1.73		11.0	13.7–7.4
Cl	512	230	190	873	380	310	Sm	245	1.89	1.26	187	4.48	4.49
		260	400–130		390	540–190			2.53	0.80–0.49		2.36	2.61–1.65
F	326	600	570	513	770	720	Eu	227	0.90	0.67	167	1.67	1.55
		570	730–330		990	1680–510			1.22	0.54–0.30		0.64	0.64–0.45
S	620	980	950	1295	620	560	Dy	230	2.54	2.25	184	4.89	4.94
		710	820–440		620	1260–390			1.80	1.58–0.93		1.36	1.61–1.22
CO_2	226	210	130	350	130	90	Er	230	1.69	1.53	175	2.66	2.64
		380	430–100		230	210–60			0.99	0.86–0.55		0.74	0.86–0.65
Be	24	0.77	0.75	32	0.85	0.88	Yb	340	1.72	1.61	186	2.22	2.22
		0.22	0.30–0.22		0.26	0.29–0.22			0.79	0.78–0.52		0.71	079–0.59
B	61	1.26	1.07	23	1.59	1.44	Hf	22	3.82	3.42	96	3.71	3.73
		1.16	1.54–0.63		0.82	0.74–0.49			1.94	2.66–1.50		0.63	0.81–0.67

Note: The contents of major elements and water are given in wt %, other elements are in ppm; *n* is the number of determinations, (arithm.) is the arithmetic mean, value below denotes the deviation from the mean; (geom.) is the geometric mean, the range of two values below show plus and minus deviation from the mean, respectively. The contents of elements were calculated as arithmetic and geometric means under the conditions that the largest deviation of individual measurements differ from the average value by no more than 2 σ with a probability 95%.

840 determinations of F, 1915 determinations of S, as well as more than 7000 determinations of nonvolatile trace elements. Major elements were analyzed by an electron microprobe. Trace and volatile elements were determined on electron and ion microprobes, by IR spectrometry, or by other methods. The accuracy of analyses for elements depends on the method employed, but this factor is not considered in this work. In our opinion, the use of a great number of diverse analytical data results in the mutual compensation of the individual systematic errors, allowing us to obtain a reliable estimate of the average melt composition. In particular, this is supported by the fact that, beginning with a certain volume of the database, the addition of even a large number of analyses only insignificantly affects the average composition and dispersion.

Available analytical data characterize various oceanic islands, plateaus, and the floor of the adjacent basins. The largest number of analyses of basic magmas is available for the Hawaiian islands (more than 600 determinations), a few tens of determinations are available for the Canary Islands, Kerguelen, Reunion, and the Ontong plateau.

The average compositions of melt inclusions and quenched glasses of the rocks are generally close to each other (Table 1), with some systematic differences. The main difference is that the inclusions have more magnesian and less differentiated compositions. This is confirmed, along with Mg contents, by the lower contents of practically all incompatible elements, including water, chlorine, and fluorine. The ratio of the average contents in rock glasses to those in inclusion glasses for most incompatible elements, including water, chlorine, and fluorine, is within 0.5–0.9. It is important that the water ratio (0.83) also falls into this interval. This indicates that the possible water loss from inclusions via hydrogen diffusion through olivine [53–56] was insignificant. Given this fact, the analyses of inclusions and quenched glasses will be considered together.

AVERAGE COMPOSITION OF OCEAN ISLAND BASIC MAGMAS

Table 2 lists the average chemical compositions of ocean-island magmatic melts, including the contents of some volatile components (water, chlorine, sulfur, and fluorine). Only compositions with SiO_2 contents no higher than 54 wt %, the main maximum of basic compositions of ocean-island magmas, were used (Fig. 1). Since the contents of most trace elements display a lognormal distribution (Fig. 2), the geometric mean is taken as the distribution maximum. In some cases, arithmetical averages are also useful in estimating the global fluxes of chemical elements. Therefore, the table displays both values with the corresponding standard deviations. It should be noted that the Ti and P distribution is close to both the normal and the lognormal distribution.

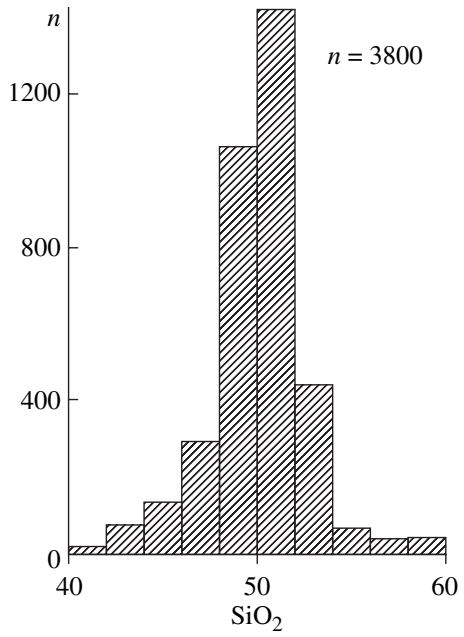

Fig. 1. Histogram of SiO_2 distribution in natural ocean-island magmatic melts, n is the number of determinations.

In Table 2, the average composition of ocean-island melts is compared with that of mid-ocean ridge melts estimated in previous work [57]. Geochemical and isotope differences between MORB and OIB basalts were repeatedly discussed in the literature, however, it will be interesting to compare their compositions using the global database of quenched melt compositions. These compositions are similar in abundance of most major elements (SiO_2, Al_2O_3, FeO, MgO, and CaO). Ocean-island magmas are significantly enriched in incompatible elements (Ti, Na, K, volatiles, and many trace elements). It should be noted that the differences between the average compositions can be related to the degree of parent melt fractionation. In particular, the insignificantly lowered Al and Mg contents in compositions of ocean islands could be interpreted as a result of olivine and plagioclase fractionation. This process can also explain some enrichment in incompatible elements. Least square calculations using major elements show that the average composition of ocean-island magmas is best approximated by the fractionation of 5% olivine and 15% plagioclase from the average MORB composition. The differences in the abundance of some compatible elements are presumably related to the crystallization of accessory phases (spinel, sulfides).

The significance of the average contents of components (C_1 and C_2) was estimated by statistical criterion $z = (C_1 - C_2)/(\sigma_1^2/n_1 + \sigma_1^2/n_2)^{1/2}$, where σ is the stan-

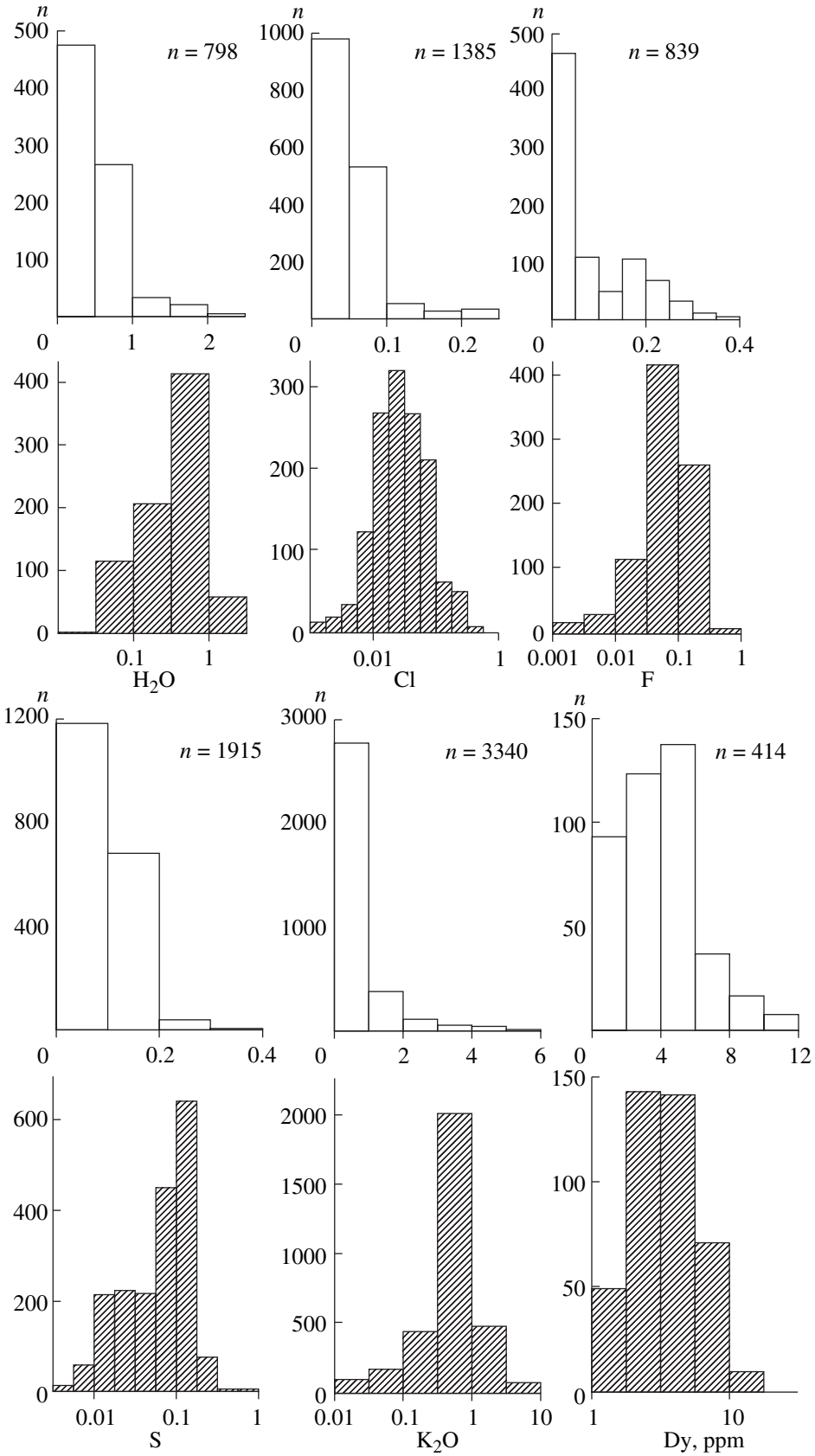

Fig. 2. Histograms of the distribution of H_2O, Cl, F, S, K_2O, Dy, P_2O_5, TiO_2, and Ce contents in ocean-island magmatic melts. Shaded histograms correspond to a lognormal distribution of elements, open histograms correspond to their normal distribution; *n* is the number of determinations.

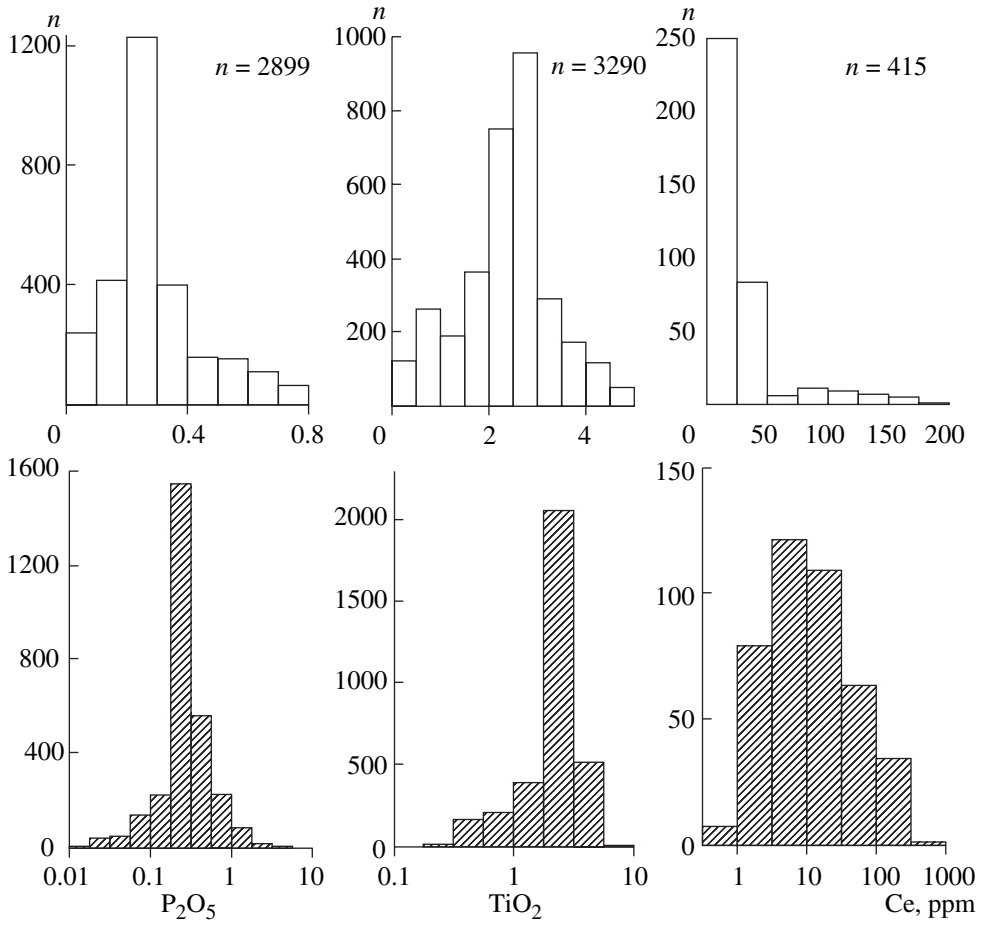

Fig. 2. (Contd.)

dard deviation and n is the number of analyses for a given component, with critical values of 2.58 for a probability of 99%. It was taken into consideration that oceanic basaltic magmas can be enriched in incompatible elements due to ~20% fractionation. As a result, we distinguished components with certainly different average concentration. As compared to the average composition of mid-ocean ridge magma, ocean-island basalts are significantly enriched in Ti, Na, K, P, Cl, and F, and, to a lesser extent, in H_2O. As a result, the average H_2O/K_2O ratio in mid-ocean ridge melts is higher than that in the melts of oceanic islands (respectively, 1.45 and 0.78). The average S content in the ocean-island magmas is approximately 25% lower than that in mid-ocean ridge melts. In addition to the most incompatible elements, ocean-island magmas are also enriched in some trace elements (Rb, Sr, Ba, Nb, Ta, Th, and U). However, this tendency is less distinct because of the wide range of compositions, especially for the melts of oceanic islands. In particular, their REE contents are overlapped even in the LREE part. With respect to moderately incompatible elements (HREE, Y, Sc), mid-ocean ridge melts are also significantly enriched relative to ocean-island basalts. It is interesting that mid-ocean ridge melts are enriched in light elements, Li and B, relative to the melts of ocean islands at practically the same Be contents.

HETEROGENEITY OF OCEAN ISLAND MAGMAS

The data reported in Table 2 indicate significant compositional variations in ocean island magmas. The fact that ocean-island melts show a greater dispersion of compositions than the melts of mid-ocean ridges was considered by many researchers as related to the heterogeneity of the mantle source [58, 59].

Our databank demonstrates that the compositions of ocean island melts are heterogeneous and display neither H_2O–K nor H_2O–Ce correlations, which were found for mid-ocean ridge melts [57]. More compact groups of magma compositions must be distinguished to estimate the heterogeneity of mantle plumes. The subdivision is based on correlations between K, Ce,

Table 2. Average contents of major, volatile, and trace elements in the magmatic melts of ocean islands and mid-ocean ridges

Component	Average composition of ocean island melts			Average composition of mid-ocean ridges			Component	Average composition of ocean island melts			Average composition of mid-ocean ridges		
	n	arithm.	geom.	*n*	arithm.	geom.		*n*	arithm.	geom.	*n*	arithm.	geom.
SiO_2	3447	50.24	50.23	3762	50.20	50.20	Sr	*493*	*259*	*232*	*803*	*135*	*130*
		2.08	2.16–2.08		0.92	0.93–0.92			257	360–140		65	62–44
TiO_2	*3290*	*2.42*	*2.04*	*2596*	*1.34*	*1.24*	Y	*361*	*20.4*	*19.6*	*796*	*28.1*	*28.0*
		0.84	0.92–0.63		0.62	0.53–0.38			12.2	17.1–9.1		13.1	12.7–8.7
Al_2O_3	3305	13.84	13.85	2525	15.59	15.58	Zr	476	92.0	83.8	929	93.7	90.2
		1.55	1.67–1.49		1.21	1.25–1.16			85.0	166–58		53.1	74.9–40.9
FeO	3341	10.72	10.66	2583	9.24	9.23	Nb	*324*	*17.4*	*10.2*	*763*	*4.84*	*2.37*
		1.91	2.27–1.87		1.65	1.71–1.43			32.3	13.0–5.7		6.89	4.36–1.54
MnO	2159	0.16	0.16	1450	0.16	0.16	Ba	*357*	*80.6*	*62.9*	*654*	*30.6*	*16.6*
		0.07	0.07–0.05		0.04	0.06–0.04			110	160–45		52.8	57.0–12.9
MgO	3424	7.30	7.33	2815	7.81	7.80	La	529	8.26	3.58	1065	5.51	4.38
		2.10	2.66–1.95		1.43	1.58–1.32			14.4	9.71–2.61		5.98	5.71–2.48
CaO	*3305*	*11.16*	*11.19*	*2525*	*11.54*	*11.54*	Ce	415	18.0	9.16	1175	12.5	11.2
		1.49	1.85–1.59		1.10	1.23–1.10			30.8	32.6–7.2		10.9	13.3–6.1
Na_2O	*3290*	*2.35*	*2.32*	*2565*	*2.67*	*2.66*	Pr	*87*	*3.84*	*4.34*	*181*	*2.12*	*1.73*
		0.64	0.59–0.47		0.57	0.64–0.51			2.06	1.53–1.16		1.69	1.35–0.76
K_2O	*3340*	*0.51*	*0.56*	*3462*	*0.20*	*0.14*	Nd	415	10.6	7.35	874	10.6	10.4
		0.50	0.52–0.27		0.27	0.30–0.10			13.4	19.7–5.4		5.9	7.0–4.2
P_2O_5	*2899*	*0.28*	*0.28*	*2243*	*0.15*	*0.14*	Sm	*432*	*3.12*	*2.35*	*952*	*3.57*	*3.45*
		0.22	0.24–0.13		0.12	0.16–0.07			3.16	4.05–1.49		1.88	1.68–1.21
H_2O	*798*	*0.40*	*0.45*	*1051*	*0.29*	*0.30*	Eu	394	1.23	0.98	793	1.28	1.21
		0.36	0.55–0.25		0.26	0.37–0.16			1.18	1.50–0.59		0.61	0.51–0.36
Cl	*1385*	*320*	*270*	*1151*	*180*	*130*	Gd	*150*	*5.86*	*5.89*	*547*	*4.42*	*4.36*
		350	510–180		260	450–100			2.18	2.33–1.67		1.46	1.55–1.14
F	*839*	*650*	*620*	*341*	*180*	*160*	Tb	39	0.93	0.91	246	0.74	0.78
		760	1130–400		170	210–90			0.29	0.22–0.18		0.26	0.27–0.20
S	1900	710	720	549	1010	990	Dy	*414*	*3.56*	*3.40*	*779*	*4.82*	*4.74*
		630	1190–450		420	480–320			2.34	3.19–1.64		2.06	2.01–1.41
CO_2	576	180	110	455	190	150	Ho	85	1.07	1.05	170	1.01	0.98
		310	330–80		210	120–70			0.13	0.12–0.11		0.34	0.34–0.25
Total		99.58	99.24		99.19	98.99	Er	*405*	*2.11*	*1.98*	*637*	*3.05*	*3.00*
T, °C	870	1194	1194	504	1227	1227			1.18	1.34–0.81		1.25	1.13–0.82
		65	66–62		42	43–42	Tm	39	0.46	0.45	173	0.41	0.40
Li	*33*	*4.51*	*4.41*	*307*	*6.33*	*6.16*			0.08	0.09–0.07		0.14	0.14–0.10
		1.47	1.36–1.04		2.22	1.82–1.40	Yb	*526*	*1.89*	*1.81*	*817*	*2.98*	*2.90*
Be	56	0.80	0.75	308	0.61	0.62			0.91	0.91–0.61		1.35	1.26–0.88
		0.25	0.51–0.30		0.38	0.38–0.24	Lu	*81*	*0.33*	*0.34*	*455*	*0.45*	*0.43*
B	*84*	*1.33*	*1.22*	*193*	*1.86*	*1.61*			0.07	0.09–0.07		0.20	0.15–0.11
		1.10	1.12–0.58		1.18	1.00–0.62	Hf	*118*	*3.56*	*3.71*	*398*	*2.39*	*2.31*
Sc	*112*	*31.9*	*32.6*	*574*	*38.5*	*38.4*			1.09	1.39–1.00		1.07	1.19–0.79
		8.6	11.9–8.7		5.3	6.0–5.1	Ta	*80*	*0.89*	*0.90*	*370*	*0.30*	*0.28*
V	262	274	262	546	269	267			0.28	0.34–0.25		0.41	0.55–0.19
		140	147–94		65	77–64	Pb	84	0.89	1.02	326	0.71	0.73
Cr	685	485	382	858	303	299			0.61	0.81–0.46		0.53	0.41–0.26
		624	690–250		198	239–133	Th	*94*	*0.64*	*0.66*	*525*	*0.46*	*0.37*
Co	44	49.8	50.4	216	44.8	44.8			0.52	1.00–0.40		0.74	0.78–0.25
		7.7	10.2–8.5		5.4	5.5–4.9	U	*84*	*0.26*	*0.21*	*397*	*0.16*	*0.10*
Ni	*317*	*226*	*176*	*399*	*97.5*	*97.5*			0.10	0.40–0.14		0.26	0.21–0.06
		220	270–110		48.0	54.2–34.8							
Rb	*155*	*10.1*	*8.61*	*500*	*4.01*	*1.53*							
		13.1	8.68–4.32		6.85	3.71–1.08							

Note: *T*, °C is the melt temperature, other symbols are as in Table 1. Italicized characters denote components whose average contents significantly differ with a probability of more than 99% with allowance for the possible different degrees of fractionation (up to 20% silicate phases and subordinate amounts of spinel and sulfide melt).

H_2O, Ti, and P contents in magmas (Fig. 3). Using the K_2O–H_2O diagram (Fig. 3a), the melt compositions can be subdivided into three groups: (I) a low-K group, (II) a high-K and low-H_2O group, and (III) a high-K and high-H_2O group. The boundary between fields I and II + III runs at 0.2 wt % K_2O, while the boundary between fields II and III corresponds to 0.2 wt % H_2O. A similar situation is observed in the TiO_2–H_2O, Ce–H_2O, and P_2O_5–H_2O diagrams (Figs. 3b–3d), but only scarce data are available for Ce. Thus, the following three main groups of ocean island basalts can be distinguished: (I) low-K basalts enriched in P and Ti and close to ocean-ridge basalts, (II) high-K basalts enriched in Ce, P, and Ti and close to continental-rift melts but differing in lower water content, and (III) high-K compositions rich in water, Ce, P, Ti and close to the continental rift melts. The average compositions of these types of magmatic melts are shown in Table 3.

The distinguished melt groups are unequally distributed between magmatic complexes presented in our database (Table 4). Only Hawaiian islands are more or less abundant in all three types. Other islands are strongly dominated by one of these types. This distribution points to a global heterogeneity of ocean-island magmatic source. At the same time, the similar average compositions of definite magma types in different complexes suggest the existence of a limited number of the geochemical types of their sources.

Figure 4 demonstrates the position of ocean-island magmas in a SiO_2–K_2O diagram. The compositions of field I in this classification diagram correspond to low-K tholeiites, while those of fields II and III are high-K subalkaline rocks that show SiO_2 decrease with increasing K_2O content. These trends are opposite to the compositional variations caused by olivine fractionation. A negative correlation between K_2O and SiO_2 is caused by variations in the degree of garnet peridotite melting at pressures higher than 30 kbar [60].

Now, let us consider the F and Cl contents in these groups. Data on F are significantly scanty than those on H_2O and Cl. It is seen that the distribution of the data points of the three groups in the F–K diagram (Fig. 5a) differs from that in the K_2O–H_2O diagram (Fig. 3a). First, the compositions of fields I, II, and high-F compositions of field III define a correlation line and overlap with the fields of mid-ocean ridges and continental rifts, except tholeiite magmas of the Hawaiian Islands [5].The average K_2O/F ratio for ocean-island basalts (Table 2) is about 9. The F content in field III strongly varies at an almost constant K_2O content. In addition, compositional fields II and III nearly coincide. Low-K melts of field I also have low F contents (<0.025 wt %) and overlap with the low-F compositions of field III. The high-K anhydrous compositions of field II are plotted in the field of high-F magmas, while high-K hydrous magmas III fall in the compositional field with wide F variations. Practically all magmas containing more than 0.05 wt % F have high K_2O content (K_2O > 0.2 wt %).

Like other components, the F and H_2O content are not correlated (Fig. 5e). Field I occupies the left, low-F part of the diagram, field II spans the low-water but high-F part of diagram, while field III occupies the high-H_2O part of the diagram with wide F variations. Figure 5c demonstrates relations between F and P_2O_5, which are close in their degree of compatibility. The K_2O/F and P_2O_5/F ratios decrease with increasing F content (Figs. 5b, 5d). It should also be noted that similar correlations are observed for mid-ocean ridge basalts (field MORB in the figures).

The variations of Cl content versus K_2O, H_2O, and F are shown in Fig. 6. In terms of contents of similarly compatible Cl and K (Fig. 6a), two groups with widely ranging Cl contents are distinguished: low-K compositions (K_2O < 0.2 wt %, mainly field I) and high-K compositions (K_2O > 0.2 wt %, fields II and III). Both of these fields form an extended ellipse overlapping with the compositional field of mid-ocean ridge magmas and high-K and high-Cl field of continental rift basaltic magmas. The K_2O/Cl ratio varies from 0.1 to more than 100 (Fig. 6d). In spite of a wide scatter in the Cl content, this dependence is statistically significant with a high probability. The high-K compositions of fields II and III (Fig. 6a) define a lower angle of the Cl–K_2O correlation than the angle of the whole sampling; the K_2O/Cl ratio varies from more than 100 to 10 in field II and from 10 to 1 in field III (Fig. 6d).

A similar correlation is also discernible for Cl and H_2O (Fig. 6b). The compositions of field I cover the practically entire interval of Cl contents in the ocean island basaltic magmas. Fields II and III define "anhydrous" and hydrous sampling sets, respectively. As a whole, the compositions of ocean-island basaltic magmas overlap with the mid-ocean ridge field and extend toward higher H_2O and Cl contents. The H_2O/Cl ratio (Fig. 6e) declines from almost 100 to less than 10 at the average ratio of 17, which is lower than that in seawater.

No significant F–Cl correlation was found for either ocean island magmas or fields I–III (Fig. 6c). However, from fields of mid-ocean ridge to continental rift basalts, most compositions show an increase in Cl and F contents. Basalts from field II widely vary in Cl at an almost constant F content.

Sulfur in ocean-island basaltic magmas shows a more complex distribution, which is presumably related to sulfide redistribution. First, S shows no correlation with Dy and other HREE, as was observed for mid-ocean ridge magmas [57]. Second, most ocean

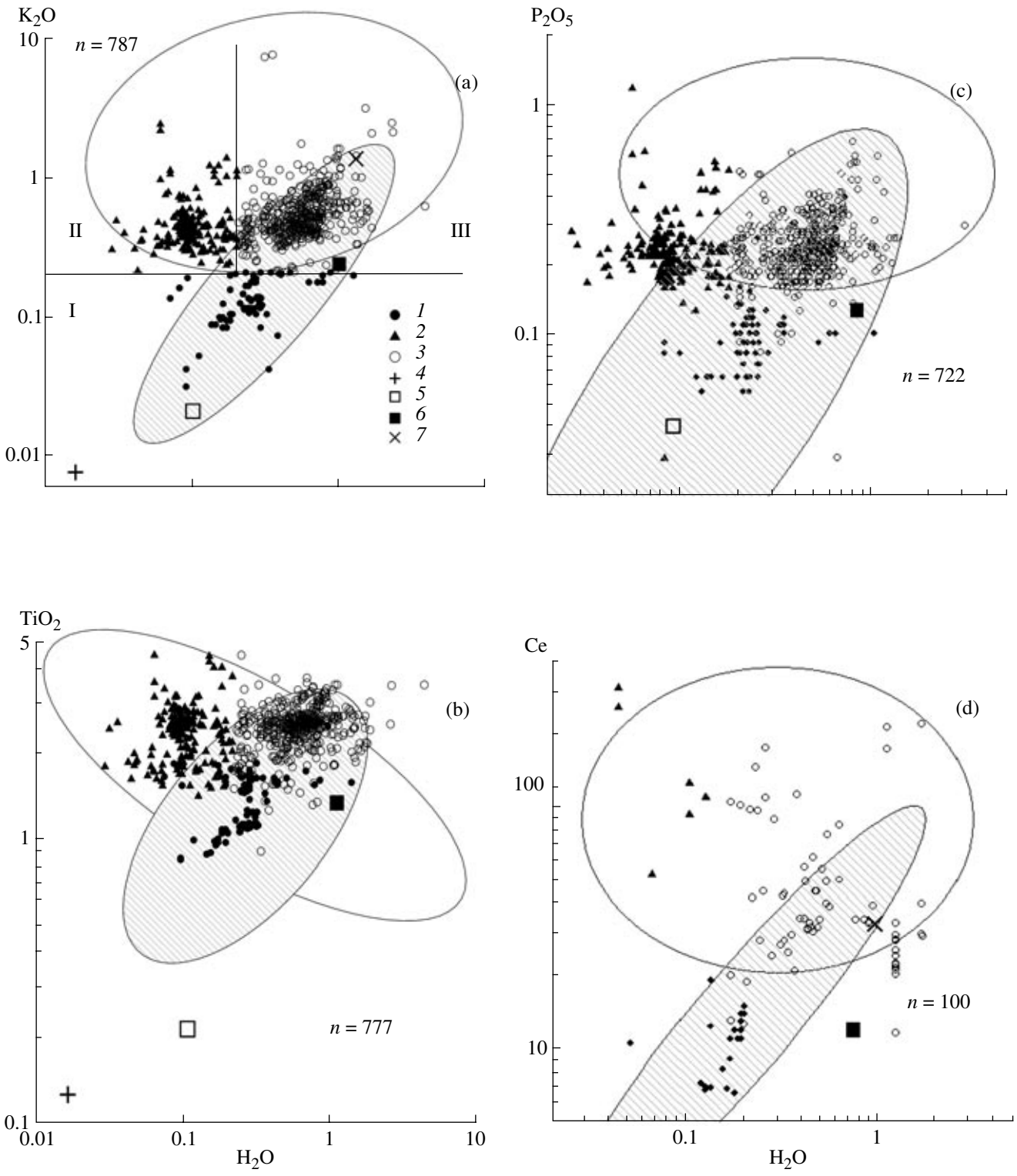

Fig. 3. Correlations between (a) K and H_2O, (b) TiO_2 and H_2O, (c) P_2O_5 and H_2O, and (d) Ce and H_2O in ocean-island magmatic melts. (*1*) Field I (low-K melts with $K_2O < 0.2$ wt %); (*2*) field II: high-K melts with $K_2O > 0.2$ wt % and low H_2O contents ($H_2O < 0.2$ wt %); (*3*) high-K melts with $K_2O > 0.2$ wt % and high $H_2O > 0.2$ wt %; (*4*) depleted mantle; (*5*) primitive mantle; (*6*) oceanic crust; (*7*) continental crust. Hereinafter, the shaded field corresponds to mid-ocean ridge melts, while the open field, to the compositions of continental rift and hot spot melts.

Table 3. Average contents of major, volatile, and trace elements in three types of ocean-island magmatic melts

Component	Average compositions of different types of magmatic melts								
	I (K_2O < 0.2 wt %)			II (K_2O > 0.2 wt %, H_2O < 0.2 wt %)			III (K_2O > 0.2 wt %, H_2O > 0.2 wt %)		
	n	arithm.	geom.	*n*	arithm.	geom.	*n*	arithm.	geom.
SiO_2	465	49.73	49.72	188	50.86	50.85	518	49.93	49.89
		1.24	1.27–1.88		1.41	1.44–1.39		2.18	2.27–2.17
TiO_2	451	0.92	0.96	184	2.44	2.46	512	2.59	2.60
		0.54	0.59–0.36		0.57	0.63–0.51		0.41	0.46–0.40
Al_2O_3	453	15.28	15.25	184	13.27	13.27	512	13.53	13.60
		1.78	2.10–1.85		0.82	0.84–0.79		1.21	1.12–1.03
FeO	453	9.03	8.99	188	11.00	11.00	518	11.17	11.02
		2.45	2.48–1.94		0.71	0.71–0.67		1.15	1.55–1.36
MnO	347	0.16	0.16	133	0.14	0.14	305	0.17	0.17
		0.05	0.07–0.05		0.06	0.06–0.04		0.03	0.03–0.03
MgO	465	8.53	8.50	188	8.31	8.14	518	7.20	7.22
		1.76	1.96–1.60		2.97	3.40–2.40		1.79	2.08–1.62
CaO	453	13.22	13.21	184	10.67	10.69	512	10.92	10.87
		1.66	1.96–1.71		1.09	1.14–1.03		1.15	1.33–1.18
Na_2O	451	1.96	1.92	184	2.33	2.33	512	2.44	2.44
		0.46	0.50–0.40		0.24	0.23–0.21		0.54	0.49–0.41
K_2O	465	0.07	0.07	188	0.41	0.40	518	0.53	0.53
		0.06	0.11–0.04		0.15	0.12–0.09		0.28	0.23–0.16
P_2O_5	359	0.09	0.08	180	0.26	0.25	470	0.27	0.27
		0.08	0.10–0.04		0.07	0.08–0.06		0.09	0.10–0.07
H_2O	81	0.24	0.24	188	0.10	0.10	518	0.55	0.62
		0.11	0.11–0.08		0.03	0.04–0.03		0.29	0.30–0.20
Cl	140	280	290	106	90	90	280	320	310
		480	2470–260		70	80–40		280	360–170
F	15	230	190	104	450	470	145	450	410
		210	260–110		220	200–150		530	860–280
S	106	1090	1060	179	370	340	412	1130	1120
		460	620–400		340	520–200		460	590–380
CO_2	66	170	100	113	100	50	385	210	120
		280	200–60		170	180–40		370	420–90
Total		99.44	99.26		99.89	99.74		99.52	99.42
T, °C	166	1255	1255	16	1208	1206	147	1165	1165
		38	38–38		94	97–89		40	40–39
Li	9	3.82	3.81	–	–	–	10	4.09	4.08
		0.46	0.48–0.43		–	–		0.40	0.42–0.38
Be	9	0.15	0.13	–	–	–	46	0.83	0.85
		0.15	0.31–0.09		–	–		0.20	0.15–0.13
B	30	0.52	0.58	–	–	–	36	1.78	1.78
		0.28	0.40–0.24		–	–		0.63	0.62–0.46
Sc	20	52.8	52.7	–	–	–	15	32.9	32.8
		4.3	4.5–4.2		–	–		3.8	3.9–3.5
V	122	230	235	6	348	343	22	282	286
		114	150–93		76	86–70		114	180–110
Cr	156	397	313	6	94.6	89.0	49	235	275
		502	380–170		106	260–66		245	560–180
Co	21	51.8	52.3	–	–	–	–	–	–
		7.5	10.4–8.7		–	–		–	–
Ni	22	79.9	78.1	–	–	–	–	–	–
		26.0	28.2 – 20.7		–	–		–	–
Rb	18	0.76	0.67	–	–	–	41	14.8	12.8
		0.72	0.26 – 0.19		–	–		11.7	9.7 – 5.5

Table 3. (Contd.)

Component	Average compositions of different types of magmatic melts								
	I (K_2O < 0.2 wt %)			II (K_2O > 0.2 wt %, H_2O < 0.2 wt %)			III (K_2O > 0.2 wt %, H_2O > 0.2 wt %)		
	n	arithm.	geom.	*n*	arithm.	geom.	*n*	arithm.	geom.
Sr	146	100	101	6	1100	1130	60	439	442
		52	57–36		1020	1240–590		205	290–175
Y	145	14.3	14.3	6	36.7	36.1	60	25.9	25.2
		9.0	11.4–6.3		10.1	11.4–8.7		8.4	9.7–7.0
Zr	146	31.9	33.4	6	439	438	60	144	149
		32.6	60.4–21.5		48	50–45		71	72–49
Nb	67	2.51	1.70	6	77.4	81.9	50	20.6	20.8
		2.65	2.65–1.04		70.2	83–41		16.4	19.0–10.0
Ba	89	15.9	12.5	6	401	401	50	155	146
		18.8	30.7–8.9		476	800–270		93	110–62
La	158	2.07	1.47	6	63.5	62.5	68	18.5	15.3
		1.85	1.63–0.77		75.0	140–43		19.2	15.3–7.66
Ce	141	5.15	4.76	6	129	134	68	41.9	36.9
		4.46	5.49–2.55		112	210–82		35.6	31.9–17.1
Pr	16	1.29	1.29	–	–	–	12	5.10	5.09
		0.08	0.08–0.08		–	–		0.56	0.60–0.54
Nd	141	4.89	4.72	6	67.7	84.0	68	22.9	22.0
		3.76	5.17–2.47		42.0	58.2–34.4		13.4	13.6–8.4
Sm	157	1.86	1.61	6	12.4	15.0	68	5.70	5.64
		1.39	1.47–0.77		5.7	8.1–5.2		2.68	3.11–2.00
Eu	141	0.75	0.67	6	3.62	4.30	50	2.06	2.07
		0.51	0.43–0.26		1.73	2.53–1.59		0.46	0.52–0.42
Gd	36	4.57	4.67	–	–	–	40	6.20	6.17
		2.91	3.83–2.10		–	–		1.49	1.57–1.26
Tb	16	0.77	0.77	–	–	–	9	1.02	1.01
		0.06	0.06–0.06		–	–		0.14	0.14–0.12
Dy	141	3.01	2.83	6	7.85	8.27	67	5.02	5.20
		2.01	2.43–1.31		2.41	3.76–2.59		1.66	1.87–1.38
Ho	16	1.12	1.12	–	–	–	12	1.07	1.06
		0.07	0.07–0.08		–	–		0.13	0.11–0.09
Er	141	1.94	1.76	6	3.80	4.00	65	2.53	2.50
		1.21	1.33–0.76		1.46	1.44–1.06		0.86	0.94–0.68
Tm	16	0.47	0.48	–	–	–	9	0.38	0.38
		0.03	0.04–0.04		–	–		0.07	0.08–0.06
Yb	157	1.80	1.64	6	3.03	3.01	68	2.09	2.16
		1.10	1.13–0.67		0.56	0.58–0.48		0.77	0.88–0.63
Lu	16	0.44	0.44	–	–	–	12	0.33	0.33
		0.03	0.04–0.04		–	–		0.06	0.06–0.05
Hf	21	1.87	1.73	–	–	–	39	4.13	4.14
		0.32	0.37–0.31		–	–		1.05	1.27–0.98
Ta	16	0.08	0.08	–	–	–	12	1.09	1.06
		0.02	0.02–0.01		–	–		0.17	0.18–0.15
Pb	20	0.26	0.30	–	–	–	12	0.78	0.98
		0.09	0.11–0.08		–	–		0.46	0.71–0.42
Th	27	0.08	0.08	–	–	–	14	1.02	0.95
		0.04	0.05–0.03		–	–		0.21	0.39–0.27
U	20	0.02	0.02	–	–	–	12	0.31	0.31
		0.02	0.04–0.01		–	–		0.05	0.06–0.05

Note: *T*, °C is the melt temperature. For other explanations, see Table 1.

island compositions is plotted below the FeO–S correlation line (Fig. 7), though many compositions are higher in S than mid-ocean ridge magmas. The bulk of ocean island melts plots in a narrow range of Fe contents (10–13 wt %) at significant variations in S content from a few hundreds ppm to 0.2 wt %. Only magma compositions from field I show a weak positive correlation of FeO with S (Fig. 7a) and a negative correlation for CaO (Fig. 7b). The prevailing part of basaltic magmas from field II is lower in S than magmas from field I, while compositions of field III are characterized by the wider variations in S content, partially overlapping with fields I and II.

In the K_2O–P_2O_5, K_2O–Ce, P_2O_5–Ti_2O, and K_2O–TiO diagrams (Fig. 8), field II overlaps field III, and all compositions of ocean island basaltic magmas define a single positive logarithmic correlations, in which field I is located in the region of low K_2O, TiO_2, and P_2O_5 contents, while fields II and III are in the region of high contents of these elements.

Table 3 lists average compositions calculated for the three aforementioned groups of ocean island melts, which can be compared with the average compositions of mid-ocean ridge melts (Table 2). Low-K basaltic rocks from field I are similar to mid-ocean ridge magmas but differ from them in lower contents of Ti, Na, K, and P and higher contents of Mg and Ca. The average compositions of fields II and III differ from that of field I in elevated contents of Ti, Fe, Na, and P. Average compositions of fields II and III differ mainly by contents of H_2O, Cl and S, with the lowest average content of H_2O, Cl, and S (but not F) occurring in field II.

Table 5 presents the average ratios of volatile and nonvolatile components in the distinguished types of ocean-island melts, which were used, together with the data of Table 2, to estimate the composition of the sources of these magmas or plume mantle. However, first we had to estimate how these compositions were modified by near-surface processes (assimilation, volatile loss, crystallization differentiation, and others). It should be noted that the dispersion's of the average contents and their ratios for three magma types are much more significant than the variations of these geochemical parameters caused by the difference between the primary (equilibrium with source) and differentiated magmas. However, first, material under consideration (melt inclusions and quenched glass) better approximates the composition of natural magmas than rocks themselves. Second, the correlations of volatiles with nonvolatiles, for instance, Cl with K, F with K and P, indicate that the behavior of incompatible novolatile and volatile components is controlled by the same processes. The most important of them are crystallization differentiation, anatectic melting, and mixing of magmas or their sources. These processes can bring about the aforementioned global correlations. Magma assimilation and degassing usually disturb correlations between the components considered here. The

Table 4. Number of determinations of melt inclusions and quenched glasses for three types of magmatic melts in different ocean islands and oceanic plateaus

Location	Type of magmatic melts		
	I	II	III
Iceland	218	31	49
Ontog Java plateau	77	–	5
Galapagos Islands	74	–	–
Hawaii	40	425	681
Kerguelen	18	–	44
Canary Islands	–	54	81
Tabuai Archipelago	–	3	18
Reunion Island	–	1	52

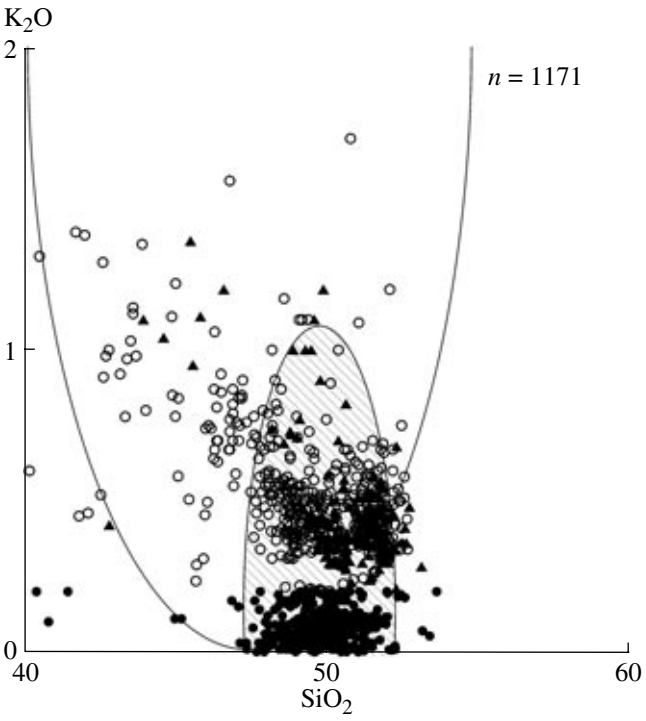

Fig. 4. Variations in the K_2O versus SiO_2 content in ocean-island magmatic melts. Symbols are shown in Fig. 3.

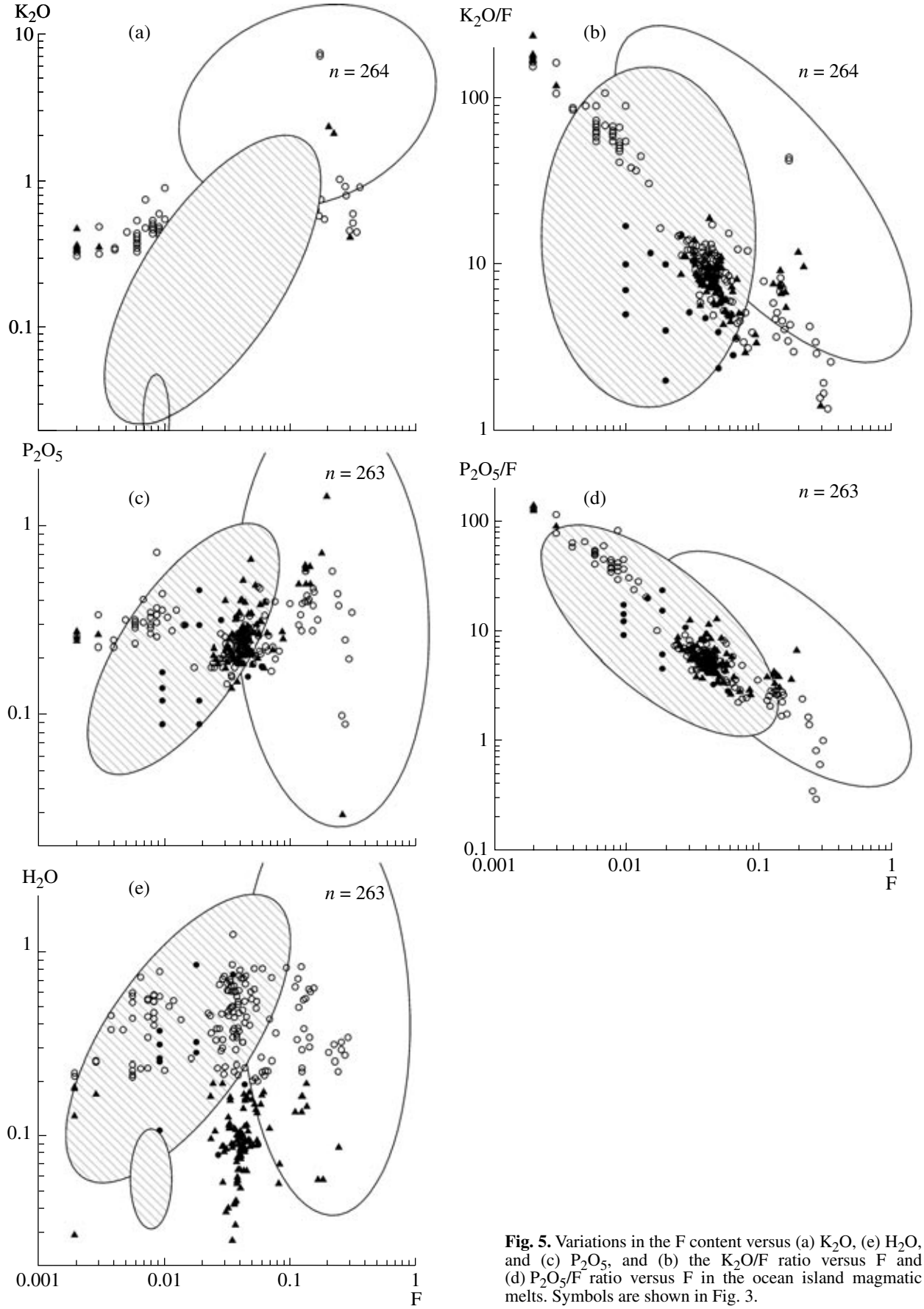

Fig. 5. Variations in the F content versus (a) K_2O, (e) H_2O, and (c) P_2O_5, and (b) the K_2O/F ratio versus F and (d) P_2O_5/F ratio versus F in the ocean island magmatic melts. Symbols are shown in Fig. 3.

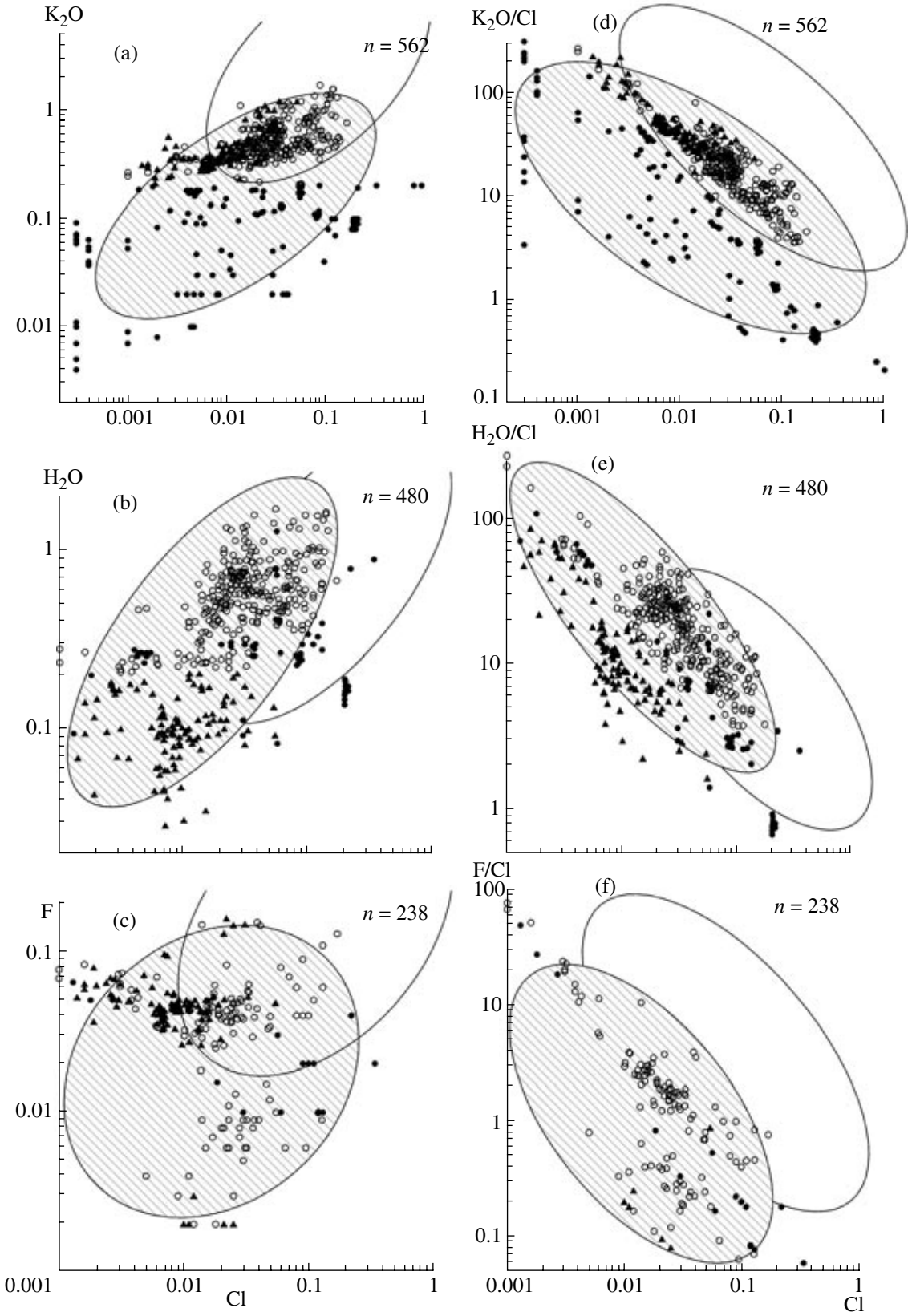

Fig. 6. Variations in the Cl content versus (a) K_2O, (b) H_2O, and (c) F, and variations in (d) K_2O/Cl ratio versus Cl, (e) H_2O/Cl ratio versus Cl, and (f) F/Cl ratio versus Cl in the ocean-island magmatic melts. Symbols are shown in Fig. 3.

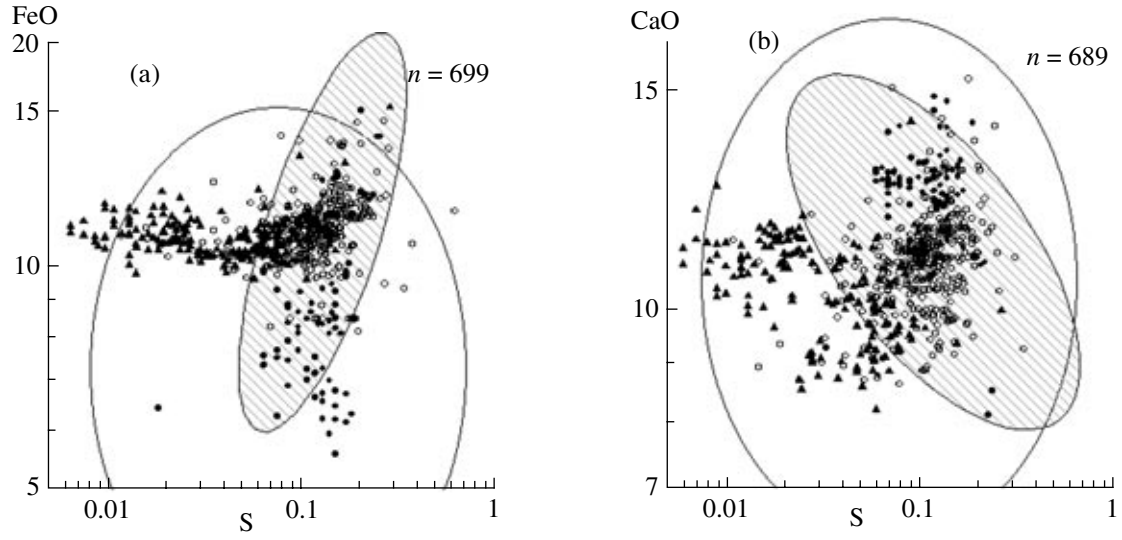

Fig. 7. Variations in the S content versus (a) FeO and (b) CaO in ocean island magmatic melts. Symbols are as in Fig. 3.

similar Mg contents of the average compositions of fields I, II, and III (Table 3) indicate that crystallization differentiation did not cause significant differences in the average contents of volatiles and in their ratios to nonvolatile components (Table 5). Conceivably, the compositions of field II could be formed by the degassing of magmas from field III (Fig. 3). However, given low water contents in the melts of field II, the degassing should occur almost at atmospheric pressure. At the same time, magmas were erupted on the seafloor at significant depths and were entrapped as melt inclusions at high pressures. Hence, magma degassing could not lead to the observed compositional difference between fields II and III. Moreover, similar K_2O–SiO_2 correlations in magmas predict the same degree of melting during the formation of the parent magmas of fields II and III (Fig. 4, Table 3). Therefore, the differences in the average contents of volatiles (Table 3) and element ratios (Table 5) are presumably related to the differences in source composition of these three magma types, i.e., the difference in mantle plume composition.

Table 5. Ratios of the average contents of components in ocean-island magmatic melts

Components	Ratios of average contents of components			
	All melts	I type	II type	III type
H_2O/Cl	17	8.3	10	19
H_2O/F	7.3	13	2.1	15
H_2O/P_2O_5	1.6	3.0	0.4	2.4
Cl/F	0.4	1.5	0.2	0.8
K_2O/H_2O	1.2	0.3	4.0	0.9
K_2O/Cl	21	2.4	40	17
K_2O/F	9.0	3.7	8.5	13
K_2O/P_2O_5	2.0	0.9	1.6	2.0
TiO_2/H_2O	4.5	4.0	25	4.2
TiO_2/Cl	76	33	250	81
TiO_2/F	33	51	52	63
TiO_2/K_2O	3.6	14	6.2	4.9
TiO_2/P_2O_5	7.3	12	9.8	10
P_2O_5/Cl	10	2.8	25	8.1
P_2O_5/F	4.5	4.2	5.3	6.3

A great number of data suggests the possibility that basaltic magmas could assimilate brines, which originated through seawater splitting into a high-density Cl-rich brine and a low-density low-Cr fluid. Therefore, it is highly possible that our sampling already contains magmas enriched in Cl due to assimilation. The low probability of this process was mentioned in [57, 61]. Nevertheless, let us estimate its probability for ocean island magmas as well as the global effect of this process on the composition of ocean-island magmas. The correlation of Cl with K_2O and H_2O shown in Fig. 6 on a logarithmic scale cannot be related to brine assimilation, because it should have led to an increase in the Cl content at a constant K_2O content and a decrease in the H_2O content, as was shown in [30, 36, and others]. The main correlation (Fig. 6) is presumably caused by the mixing of two magmatic sources: one low-Cl, low-K, and low-H_2O, and others, rich in these components [61]. The assimilation of Cl-rich seawater components by ocean-island magmas could lead to a wide scatter (within two orders of magnitude) in the Cl content at

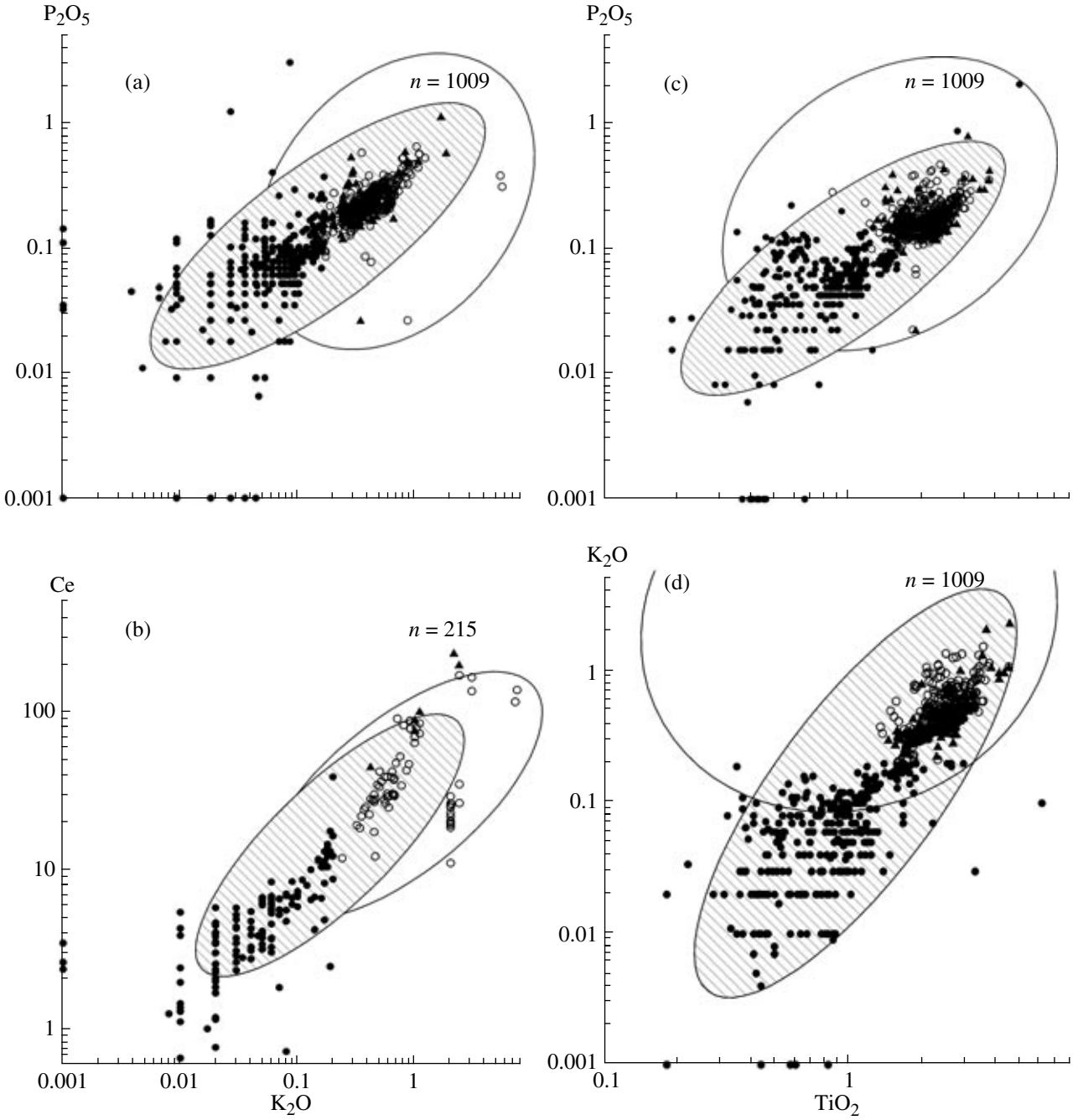

Fig. 8. Diagrams (a) K_2O–P_2O_5, (b) Ce–K_2O, (c) TiO_2–P_2O_5, and (d) TiO_2–K_2O in ocean island magmatic melts. Symbols are as in Fig. 3.

a constant content of K_2O, within the scope of the general correlation (Fig. 6a), thus causing an overestimation of the average Cl content in ocean island magmas. However, the question arises as to why the assimilation of seawater components causes the global accumulation of magma compositions around their average composition or the correlation line in Fig. 6 instead of an even and random scatter. The doubt also stems from the analysis of the Cl–K_2O correlation in the magmas of fields II and III (Fig. 6). This correlation is steeper than the general correlation for all compositions and could be explained by a significant role of Cl assimilation, leading us to admit that this process is responsible for the transition from field II to field III. This is hardly possible, since such transition requires an increase in the contents of K_2O, H_2O, S, and, possibly, Ti (Table 5).

It should be noted that the Cl content in magmas from field III occasionally reaches 2 wt % at low contents of incompatible elements, which underlay fairly exotic models proposed to account for the formation of such magmas, for instance, the anatexis of oceanic crust under NaCl brine saturation [36]. We believe that these problems can be resolved by uneven distribution of Cl, K, H_2O, and other components in the plume mantle rather than by shallow-depth seawater assimilation by magma. We admit that this heterogeneity can occur not only on the scale of large domains of mantle plumes, which characterizes the main correlation in Fig. 6, but also on a smaller scale, especially for Cl. This was demonstrated for melt inclusions in such typical within-plate magmas as NaCl-rich kimberlites [62], for the Cl balance in subduction zones [63], and for Cl isotope composition of oceanic basalts [64], which indicates that no less than 70 wt % Cl of the altered oceanic crust participates in deep-seated mantle recycling. In this context, we arrived at the conclusion that the three distinguished types of basaltic magmas characterizes three types of mantle plume sources, while the compositional variations of these magmas shown in Fig. 3 reflect the heterogeneity of the mantle sources.

CONCLUSIONS

The ultimate aim of generalizing data on ocean island magmas is to estimate the composition and chemical structure of mantle plumes, which will be considered in our ongoing paper. The results presented in this publication are the factual basis for subsequent modeling, and the most important of them are as follows:

(1) With regard for the insignificant difference in the degree of differentiation, the compositions of melts in inclusions in mineral and in quenched glasses can be considered identical, including the content of water and other volatiles.

(2) The average compositions of ocean-island magmas differ from those of mid-ocean ridge magmas in contents and ratios of some incompatible elements. At the same time, the corresponding compositional fields significantly overlap.

(3) Based on the K_2O–H_2O correlation, three types of ocean island magmas are distinguished. These types also differ with respect to other volatiles and trace elements. It is suggested that these differences are related to the existence of several geochemically distinct magma sources.

(4) The distinguished geochemical melt types are unevenly distributed in space. In particular, the Hawaii Archipelago contains all three types, whereas all other considered complexes are strongly dominated by only one of them.

ACKNOWLEDGMENTS

This study was supported by the Russian Foundation for Basic Research (project nos. 04-05-65123, 05-05-64175), the Federal Program for the Support of the Leading Scientific Schools (project nos. 1145.2003.5 and 1618.2003.5), and Program no. 5 of the Department of Earth Sciences, Russian Academy of Sciences.

REFERENCES

1. V. B. Naumov, V. I. Kovalenko, V. V. Yarmolyuk, and V. A. Dorofeeva, "Volatile Components (H_2O, Cl, F, S, and CO_2) in Magmatic Melts of Various Geodynamic Environments," Geokhimiya, No. 5, 555–564 (2000) [Geochem. Int. **38**, 500–509 (2000)].
2. V. B. Naumov, V. I. Kovalenko, V. A. Dorofeeva, and V. V. Yarmolyuk, "Average Concentrations of Major, Volatile, and Trace Elements in Magmas of Various Geodynamic Settings," Geokhimiya, No. 10, 1113–1124 (2004) [Geochem. Int. **42**, 977–987 (2004)].
3. A. R. Philpotts, "Compositions of Immiscible Liquids in Volcanic Rocks," Contrib. Mineral. Petrol. **80**, 201–218 (1982).
4. J. D. Devine, H. Sigurdsson, A. N. Davis, and S. Self, "Estimates of Sulfur and Chlorine Yield to the Atmosphere from Volcanic Eruptions and Potential Climatic Effects," J. Geophys. Res. **89** (B7), 6309–6325 (1984).
5. M. O. Garcia, D. W. Muenow, K. E. Aggrey, and J. R. O'Neil, "Major Element, Volatile, and Stable Isotope Geochemistry of Hawaiian Submarine Tholeiitic Glasses," J. Geophys. Res. **94** (B8), 10525–10538 (1989).
6. D. A. Clague, R. T. Holcomb, J. M. Sinton, et al., "Pliocene and Pleistocene Alkalic Flood Basalts on the Seafloor North of the Hawaiian Islands," Earth Planet. Sci. Lett. **98**, (2) 175–191 (1990).
7. J. E. Dixon, D. A. Clague, and E. M. Stolper, "Degassing History of Water, Sulfur, and Carbon in Submarine Lavas from Kilauea Volcano, Hawaii," J. Geol. **99** (3), 371–394 (1991).
8. A. T. Anderson and G. G. Brown, "CO_2 Contents and Formation Pressures of Some Kilauean Melt Inclusions," Am. Mineral. **78** (7-8), 794–803 (1993).
9. C. W. Sinton, D. M. Christie, V. L. Coombs, et al., "Near-Primary Melt Inclusions in Anorthite Phenocrysts from the Galapagos Platform," Earth Planet. Sci. Lett. **119**, 527–537 (1993).
10. A. V. Sobolev and I. K. Nikogosyan, "Magmatic Petrology of the Long-Lived Mantle Jets: Hawaii Islands (Pacific Ocean) and Reunion Island (Indian Ocean)," Petrologiya **2** (2), 131–168 (1994).
11. P. J. Wallace and I. S. E. Carmichael, "S Speciation in Submarine Basaltic Glasses as Determined by Measurements of S*Ka*] X-Ray Wavelength Shifts," Am. Mineral. **79** (1-2), 161–167 (1994).
12. D. A. Clague, J. G. Moore, J. E. Dixon, and W. B. Friesen, "Petrology of Submarine Lavas from Kilauea's Puna Ridge, Hawaii," J. Petrol. **36** (2), 299–349 (1995).
13. M. O. Garcia, "Petrography and Olivine and Glass Chemistry of Lavas from the Hawaii Scientific Drilling Project," J. Geophys. Res. **101** (B5), 11701–11713 (1996).

14. Th. Thordarson, S. Self, N. Oskarsson, and T. Hulsebosch, "Sulfur, Chlorine, and Fluorine Degassing and Atmospheric Loading by the 1783-1784 AD Laki (Skaftar Fires) Eruption in Iceland," Bull. Volcanol. **58** (2-3), 205–225 (1996).
15. A. A. Gurenko and M. Chaussidon, "Boron Concentrations and Isotopic Composition of the Icelandic Mantle: Evidence from Glass Inclusions in Olivine," Chem. Geol. **135** (1-2), 21–34 (1997).
16. E.-R. Neumann and E. Wulf-Pedersen, "The Origin of Highly Silicic Glass in Mantle Xenoliths from the Canary Islands," J. Petrol. **38** (11), 1513–1539 (1997).
17. H. Bureau, N. Metrich, F. Pineau, and M. P. Semet, "Magma-Conduit Interaction at Piton de la Fournaise Volcano (Reunion Island): A Melt and Fluid Inclusion Study," J. Volcanol. Geotherm. Res **84** (1-2), 39–60 (1998).
18. H. Bureau, F. Pineau, N. Metrich, et al., "A Melt and Fluid Inclusion Study of the Gas Phase at Piton de la Fournaise Volcano (Reunion Island)," Chem. Geol. **147** (1-2), 115–130 (1998).
19. A. A. Gurenko, T. H. Hansteen, and H.-U. Schmincke, "Melt, Crystal, and Fluid Inclusions in Olivine and Clinopyroxene Phenocrysts from the Submarine Shield Stage Hyaloclastites of Gran Canaria, Sites 953 and 956," Proc. ODP Sci. Results **157**, 375–401 (1998).
20. A. A. Gurenko and H.-U. Schmincke, "Geochemistry of Sideromelane and Felsic Glass Shards in Pleistocene Ash Layers at Sites 953, 954, and 956," Proc. ODP. Sci. Res. **157**, 421–428 (1998).
21. A. A. Gurenko and H.-U. Schmincke, "Petrology, Geochemistry, S, CI, and F Abundances, and S Oxidation State of Sideromelane Glass Shards from Pleistocene Ash Layers North and South of Gran Canaria (ODP Leg 157)," Contrib. Mineral. Petrol. **131** (1), 95–110 (1998).
22. T. H. Hansteen and A. A. Gurenko, "Sulfur, Chlorine, and Fluorine in Glass Inclusions in Olivine and Clinopyroxene from Basaltic Hyaloclastites Representing the Gran Canaria Shield Stage at Sites 953 and 956," Proc. ODP Sci. Results **157**, 403–410 (1998).
23. A. J. R. Kent, M. D. Norman, I. D. Hutcheon, and E. M. Stolper, "Assimilation of Seawater-Derived Components in an Oceanic Volcano: Evidence from Matrix Glasses and Glass Inclusions from Loihi Seamount, Hawaii," Chem. Geol. **156** (1-4), 299–319 (1999).
24. P. J. Michael, "Implications for Magmatic Processes at Ontong Java Plateau from Volatile and Major Element Contents of Cretaceous Basalt Glasses," Geochem. Geophys. Geosyst. **1** (1999).
25. P. Schiano and B. Bourdon, "On the Preservation of Mantle Information in Ultramafic Nodules: Glass Inclusions within Minerals versus Interstitial Glasses," Earth Planet. Sci. Lett. **169**, 173–188 (1999).
26. E. Wulff-Pedersen, E.-R. Neumann, R. Vannucci, et al., "Silicic Melts Produced by Reaction Between Peridotite and Infiltrating Basaltic Melts: Ion Probe Data on Glasses and Minerals in Veined Xenoliths from La Palma, Canary Islands," Contrib. Mineral. Petrol. **137**, 59–82 (1999).
27. D. A. Clague, A. S. Davis, J. L. Bischoff, et al., "Lava Bubble-Wall Fragments Formed by Submarine Hydrovolcanic Explosions on Lo'ihi Seamount and Kilauea Volcano," Bull. Volcanol. **61**, 437–449 (2000).
28. A. A. Gurenko and H.-U. Schmincke, "S Concentrations and Its Speciation in Miocene Basaltic Magmas North and South of Gran Canaria (Canary Islands): Constraints from Glass Inclusions in Olivine and Clinopyroxene," Geochim. Cosmochim. Acta **64** (13), 2321–2337 (2000).
29. H. Hansen and K. Gronvold, "Plagioclase Ultraphyric Basalts in Iceland: The Mush of the Rift," J. Volcanol. Geotherm. Res. **98** (1-4), 1–32 (2000).
30. J. E. Dixon and D. A. Clague, "Volatile in Basaltic Glasses from Loihi Seamount, Hawaii: Evidence for a Relatively Dry Plume Component," J. Petrol. **42** (3), 627–654 (2001).
31. L. Slater, D. McKenzie, K. Gronvold, and N. Shimizu, "Melt Generation and Movement beneath Theistareykir, NE Iceland," J. Petrol. **42**, 321–354 (2001).
32. I. P. Solovova, A. V. Girnis, I. D. Ryabchikov, and N. N. Kononkova, "Melts of the Post-Shield Stage of Mauna Kea Volcano, Hawaii: Evidence from Inclusions in Minerals of the High-Mg Basalt," Geokhimiya, No. 12, 1271–1287 (2002) [Geochem. Int. **40**, 1146–1161 (2002)].
33. M. L. Frezzotti, T. Andersen, E.-R. Neumann, and S. L. Simonsen, "Carbonatite Melt–CO_2 Fluid Inclusions in Mantle Xenoliths from Tenerife, Canary Islands: a Story of Trapping, Immiscibility and Fluid-Rock Interaction in the Upper Mantle," Lithos **64** (3-4), 77–96 (2002).
34. E. Hauri, "SIMS Analysis of Volatiles in Silicate Glasses, 2: Isotope and Abundances in Hawaiian Melt Inclusions," Chem. Geol. **183** (1-4), 115–141 (2002).
35. D. J. Kontak, De Young M. Y., De Wolfe and J. Dostal, "Late-Stage Crystallization History of the Jurassic North Mountain Basalt, Nova Scotia, Canada. I. Textural and Chemical Evidence for Pervasive Development of Silicate-Liquid Immiscibility," Can. Mineral. **40** (5), 1287–1311 (2002).
36. J. C. Lassiter, E. H. Hauri, I. K. Nikogosian, and H. G. Barsczus, "Chlorine-Potassium Variations in Melt Inclusions from Raivavae and Rapa, Austral Islands: Constraints on Chlorine Recycling in the Mantle and Evidence for Brine-Induced Melting of Oceanic Crust," Earth Planet. Sci. Lett. **202** (3-4), 525–540 (2002).
37. I. K. Nikogosian, T. Elliott, and J. L. R. Touret, "Melt Evolution beneath Thick Lithosphere: a Magmatic Inclusion Study of La Palma, Canary Island," Chem. Geol, **183**, 169–193 (2002).
38. M. D. Norman, M. O. Garcia, V. S. Kamenetsky, and R. L. Nielsen, "Olivine-Hosted Melt Inclusions in Hawaiian Picrites: Equilibration, Melting, and Plume Source Characteristics," Chem. Geol. **183**, 143–168 (2002).
39. P. J. Wallace, "Volatiles in Submarine Glasses from the Northern Kerguelen Plateau (ODP Site 1140): Implications for Source Region Compositions, Magmatic Processes, and Plateau Subsidence," J. Petrol. **43**, 1311–1326 (2002).
40. M. G. Davis, M. O. Garcia, and P. Wallace, "Volatiles in Glasses from Mauna Loa Volcano, Hawai'I: Implications for Magma Degassing and Contamination, and

Growth of Hawaiin Volcanoes," Contrib. Mineral. Petrol. **144**, 570–591 (2003).

41. M. O. Garcia, A. J. Pietruszka, and J. M. Rhodes, "A Petrologic Perspective of Kilauea Volcano's Summit Magma Reservoir," J. Petrol. **44**, 2313–2339 (2003).
42. K. S. Harpp, D. J. Fornari, D. J. Geist, and M. D. Kurz, "Genovesa Submarine Ridge: A Manifestation of Plume-Ridge Interaction in the Northern Galapagos Islands," Geochem. Geophys. Geosyst. **4**, 1–27 (2003).
43. J. Maclennan, D. McKenzie, K. Gronvold, et al., "Melt Mixing and Crystallization under Theistareykir, Northeast Iceland," Geochem. Geophys. Geosystems **4**, 1–40 (2003).
44. J. Maclennan, D. McKenzie, F. Hilton, et al., "Geochemical Variability in a Single Flow from Northern Iceland," J. Geophys. Res. **108** (B1), 1–21 (2003).
45. V. A. Simonov, V. V. Zolotukhin, S. V. Kovyazin, et al., "Petrogenesis of Basaltic Series of the Ontong Java Oceanic Plateau and the Nauru Basin, Pacific Ocean," Petrologiya **12**, 191–205 (2004) [Petrology **12**, 163–175 (2004)].
46. M. L. Coombs, T. W. Sisson, and J.-I. Kimura, "Ultra-High Chlorine in Submarine Kilauea Glasses: Evidence for Direct Assimilation of Brine by Magma," Earth Planet. Sci. Lett. **217**, 297–313 (2004).
47. E. H. Haskins and M. O. Garcia, "Scientific Drilling Reveals Geochemical Heterogeneity within the Ko'olau Shield, Hawai'i," Contrib. Mineral. Petrol. **147**, 162–188 (2004).
48. K. Kobayashi, R. Tanaka, T. Moriguti, et al., "Lithium, Boron, and Lead Isotope Systematics of Glass Inclusions in Olivines from Hawaiian Lavas: Evidence for Recycled Components in the Hawaiian Plume," Chem. Geol. **212**, 143–161 (2004).
49. M. D. Norman, M. O. Garcia, and V. C. Bennett, "Rhenium and Chalcophile Elements in Basaltic Glasses from Ko'olau and Moloka'i Volcanoes: Magmatic Outgassing and Composition of the Hawaiian Plume," Geochim. Cosmochim. Acta **68**, 3761–3777 (2004).
50. Z-Y. Ren, E. Takahashi, Y. Orihashi, and K. T. M. Johnson, "Petrogenesis of Tholeiitic Lavas from the Submarine Hana Ridge, Haleakala Volcano, Hawaii," J. Petrol. **45**, 2067–2099 (2004).
51. E. Stolper, S. Sherman, M. Garcia, et al., "Glass in the Submarine Section of the HSDP2 Drill Core, Hilo, Hawaii," Geochem. Geophys. Geosystems **5**, 1–67 (2004).
52. N. A. Stroncik and K. M. Haase, "Chlorine in Oceanic Intraplate Basalts: Constraints on Mantle Source and Recycling Processes," Geology **32**, 945–948 (2004).
53. Z. Quin, F. Lu, and A. T. Anderson, "Diffusive Re-Equilibration of Melt and Fluid Inclusions," Am. Mineral. **77**, 565–576 (1992).
54. A. V. Sobolev and L. V. Danyushevsky, "Petrology and Geochemistry of Boninites from the North Termination of the Tonga Trench: Constraints on the Generation Conditions of Primary High Ca Bonitite Magmas," J. Petrol. **35**, 1183–1211 (1994).
55. D. Massare, N. Metrich, and R. Clocchiatti, "High-Temperature Experiments on Silicate Melt Inclusions in Olivine at 1 Atm: Inference on Temperatures of Homogenization and H_2O Concentrations," Chem. Geol. **183**, 87–98 (2002).
56. E. Hauri, "SIMS Analysis of Volatiles in Silicate Glasses, 2: Isotopes and Abundances in Hawaiian Melt Inclusions," Chem. Geol. **183**, 115–141 (2002).
57. V. I. Kovalenko, V. B. Naumov, A. V. Girnis, et al., "Estimation of the Average Contents of H_2O, Cl, F, and S in the Depleted Mantle on the Basis of the Compositions of Melt Inclusions and Quenched Glasses of Mid-Ocean Ridge Basalts," Geokhimiya, No. 3, 243–266 (2006) [Geochem. Int. **44**, 209–231 (2006)].
58. A. W. Hofmann and W. M. White, "Mantle Plumes from Ancient Oceanic Crust," Earth Planet. Sci. Lett **57** (2), 421–436 (1982).
59. A. Zindler and S. Hart, "Chemical Geodynamics," Annu. Rev. Earth Planet. Science **14**, 493–571 (1986).
60. M. J. Walter, "Melting of Garnet Peridotite and the Origin of Komatiite and Depleted Lithosphere," J. Petrol. **39**, 29–60 (1998).
61. V. I. Kovalenko, V. B. Naumov, V. V. Yarmolyuk, et al., "Balance of H_2O and Cl between the Earth's Mantle and Outer Shells," Geokhimiya, No. 10, 1041–1070 (2002) [Geochem. Int. **40**, 943–971 (2002)].
62. M. B. Kamenetsky, A. V. Sobolev, V. S. Kamenetsky, et al., "Kimberlite Melts Rich in Alkali Chlorides and Carbonates: A Potent Metasomatic Agent in the Mantle," Geology **32**, 845–848 (2004).
63. P. Philippot, P. Agrinier, and M. Scambelluri, "Chlorine Cycling during Subduction of Altered Oceanic Crust," Earth Planet. Sci. Lett. **161**, 33–44 (1998).
64. A. G. Magenhein, A. G. Spivack, P. J. Michael, and J. M. Gieskes, "Chlorine Stable Isotope Composition of the Oceanic Crust: Implication for the Earth's Distribution of Chlorine," Earth Planet. Sci. Lett. **131** (3-4), 427–432 (1995).